Electronic Supplementary Material (ESI) for Photochemical & Photobiological Sciences.


# Turn on Fluorogenic Chemosensor for $Fe^{3+}$ and Schottky Barrier Diode with Frequency Switching Device Applications.

Habib Ali Molla[a], Rahul Bhowmick[a], Abu Saleh Musha Islam[a], Bibhutibhushan Show[a], Nillohit Mukherjee[b], Anup Mondal[c] and Mahammad Ali,* [a]

[a]Department of Chemistry, Jadavpur University, 188, Raja Subodh Chandra Mallick Rd, Kolkata, West Bengal 700032, India, m_ali2062@yahoo.com

[b]Centre of Excellence for Green Energy and Sensor Systems, Indian Institute of Engineering Science and Technology, Shibpur, Howrah 711103, Botanic Garden, Howrah 711103, India

[c]Department of Chemistry, Indian Institute of Engineering, Science and Technology, Shibpur, Botanic Garden, Howrah 711103, India

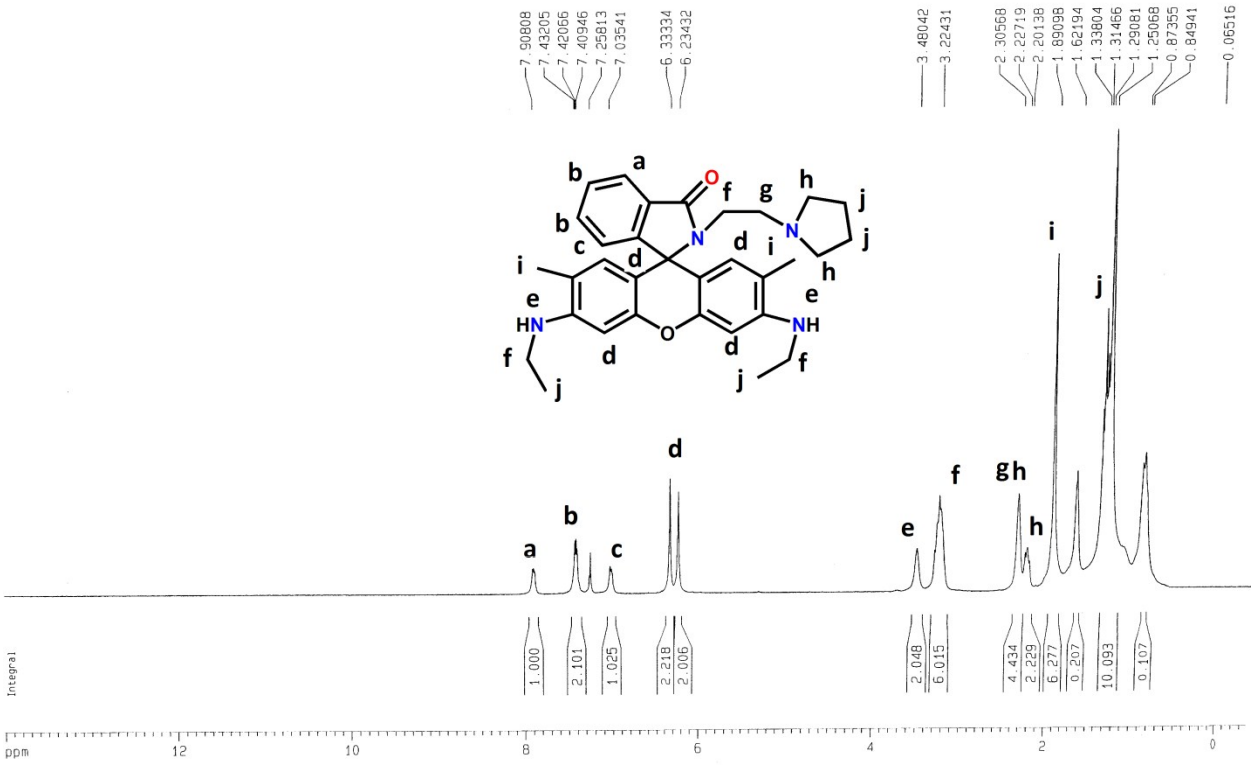


**Figure S1.** $^{1}H$ NMR spectra of L in $CDCl_3$ in Bruker 300 MHz instrument.

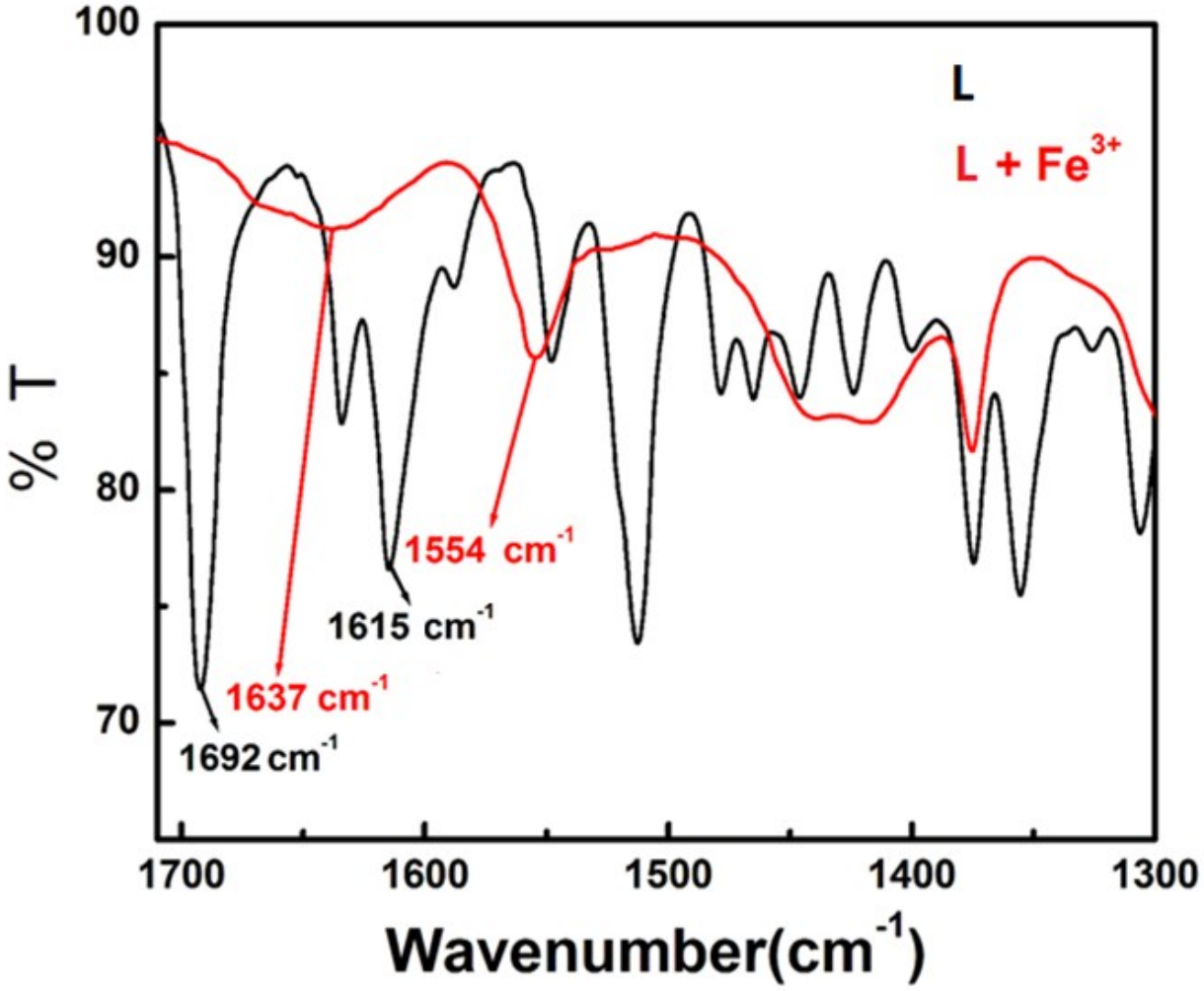


**Figure S2.** IR Spectrum of **L** and **L**-$Fe^{3+}$ complex

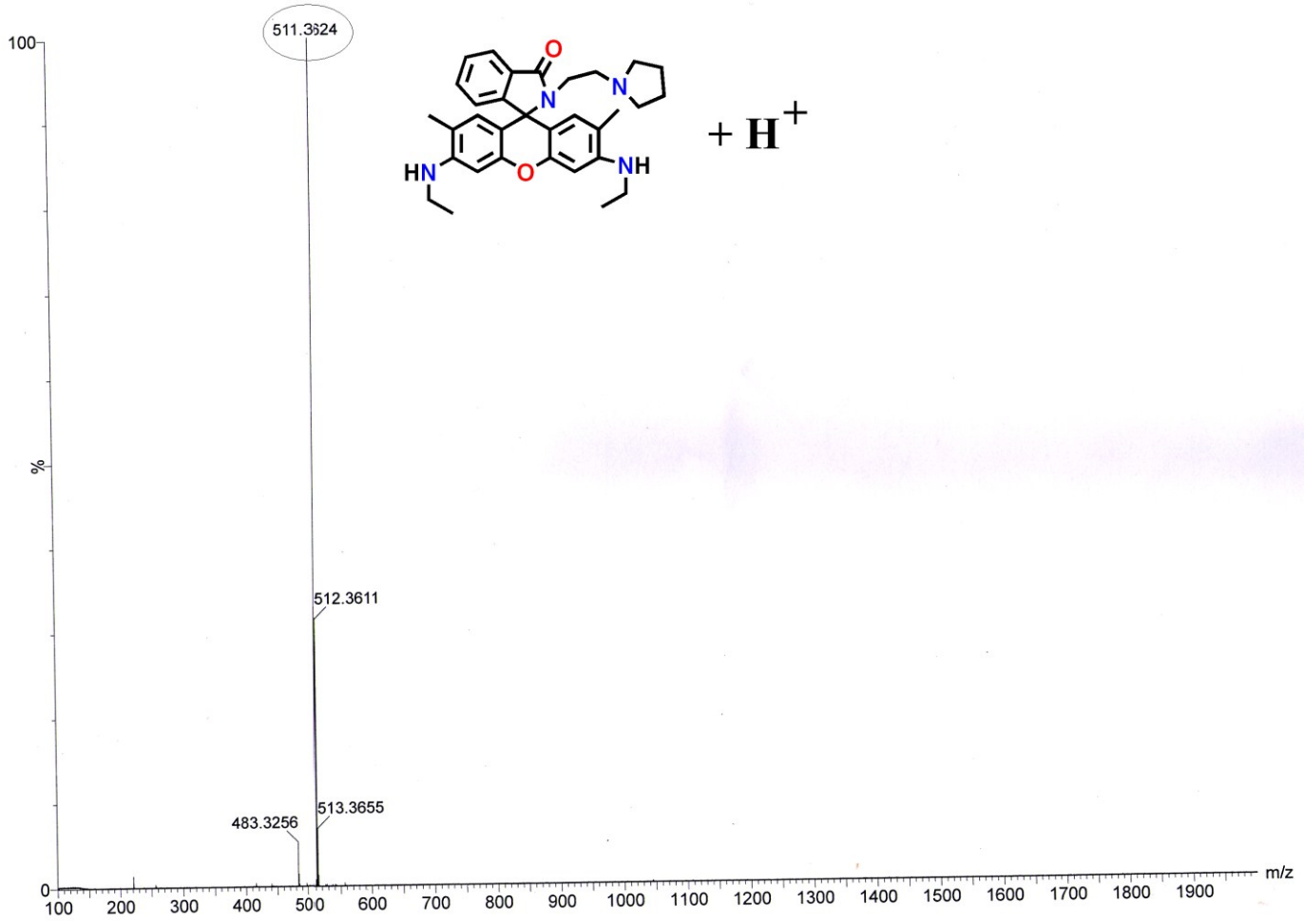


**Figure S3.** Mass spectra of L in MeCN.

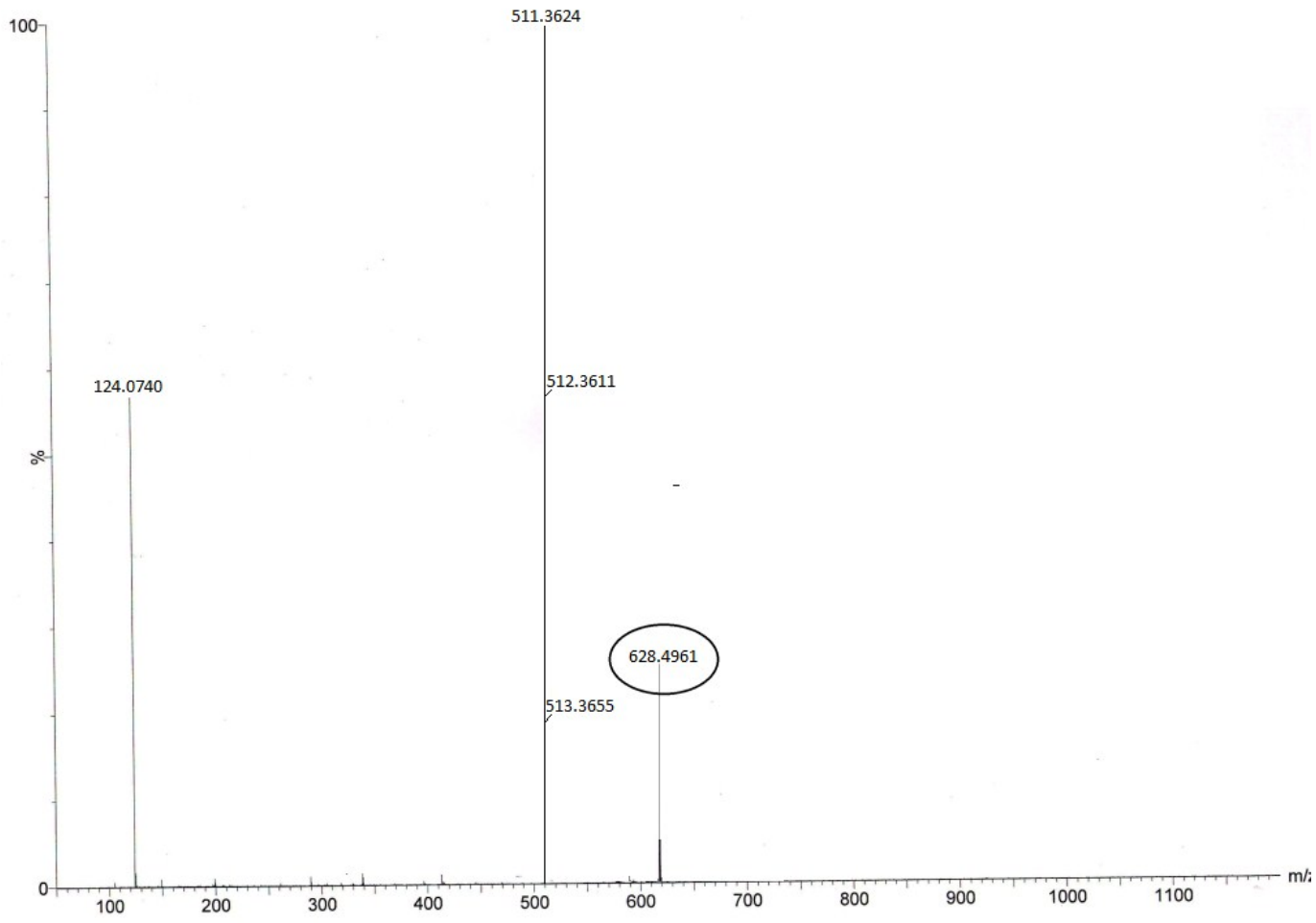


**Figure S4.** Mass spectra of **L**-$Fe^{3+}$ complex in MeCN.

**Single-crystal X-ray diffraction studies**.

Intensity data for **L²** were collected at 293(2) K on a Bruker SMART APEX-II CCD diffractometer using graphite monochromated Mo-Kα radiation (λ = 0.71073 Å and the *ω–2*θ scan mode in the range 1.8< 2θ < 26.8°). No decomposition of the crystal occurred during the data collection. The intensities were corrected for Lorentz and polarization effects and for absorption using the *ψ*-scan method. The cell parameters were refined from all strong reflections. The data reductions were carried out using the CrysAlis RED (Oxford Diffraction, UK) program, and analytical absorption corrections were applied. The

structure was determined by direct methods using SHELXS-97 and refined anisotropically on $F^2$ using the full matrix least-squares procedure of SHELXL-97. The crystallographic data for $L^2$ are given in **Table S1**.

**Table S1**. Details of crystallographic data collection and refinements

| | |
|---|---|
| Elemental formula | C32 H40 N4 O3 |
| Formula weight | 528.68 |
| Crystal system | Triclinic |
| Space group | P-1 |
| Temp/K | 296 (2) |
| a/Å | 10.36 (15) |
| b/Å | 11.54 (17) |
| c/Å | 12.54 (19) |
| V/$A^3$ | 1452.4 (4) |
| Z | 2 |
| Cell angle alpha | 81.87 (5) |
| Cell angle beta | 77.71 (5) |
| Cell angle gamma | 87.24 (5) |
| Theta min | 1.68 |
| Theta max | 27.16 |
| Crystal description | Block shape |
| Crystal colour | Light brown |
| F000 | 568.0 |
| F000' | 568.22 |
| h, k, l max | 13, 14, 16 |
| Tmin | 0.991 |
| Tmax | 0.994 |

**Solution preparation for UV-Vis and fluorescence studies**

For both UV-Vis and fluorescence titrations, a 1.0 x $10^{-3}$ M stock solution of the probe **L** was prepared by dissolving it in 0.5 ml MeCN, the volume of which was finally adjusted to 10 ml by MeCN. Similarly, 10 ml 1.0 x $10^{-3}$ M stock solution of $Fe^{3+}$ was prepared separately in MeCN. 100 ml 10 mM HEPES buffer was prepared in Milli-Q Millipore water and pH was adjusted to 7.24 by using HCl and NaOH. 2.5 ml of this buffer solution was pipetted out into a cuvette to which 50 μM of the probe was added and $Fe^{3+}$ was added incrementally starting from 0 to 80 μM in a regular interval of volume and UV-Vis spectra were recorded for each solution. For fluorescence spectra 10 μM L was added to 2.5 ml buffer solution in a cuvette and $Fe^{3+}$ was added incrementally starting from 0 to 25 μM in a regular interval of volume and fluorescence spectra were recorded for each solution. The 1 cm path lengths of the cells were used for absorption and emission studies. Fluorescence measurements were performed using 2 nm x 2 nm slit width.

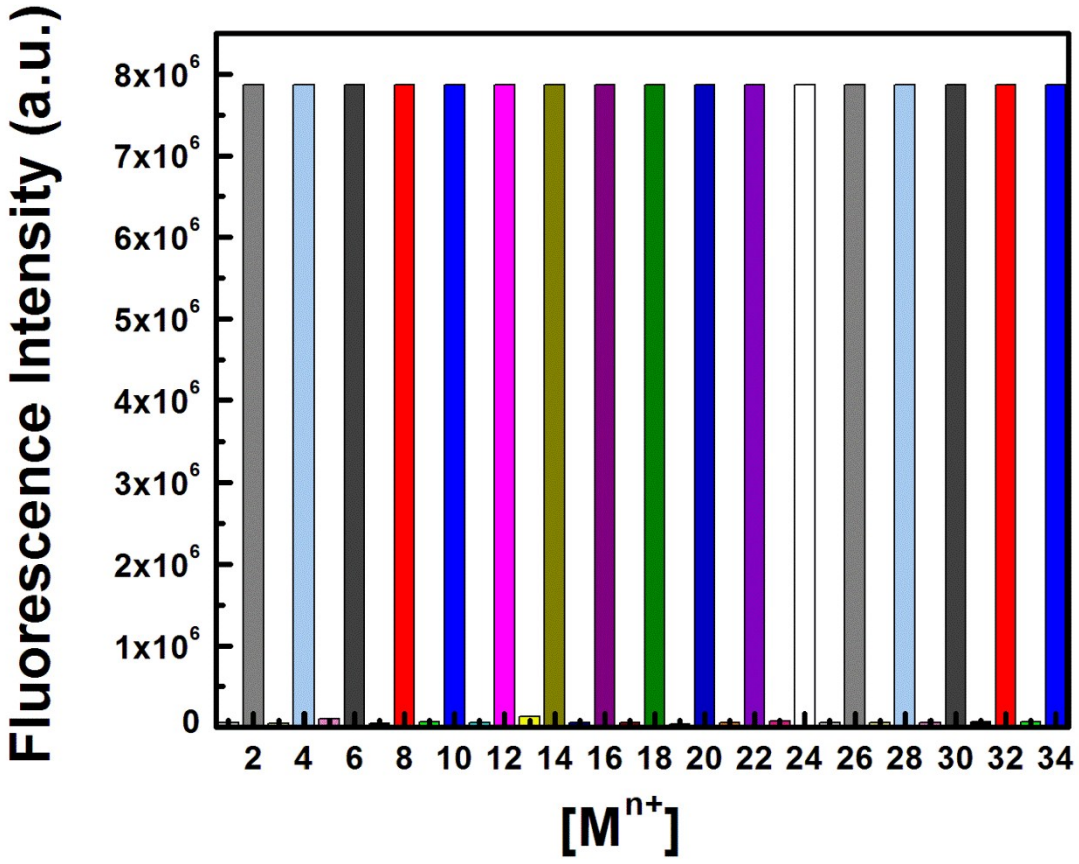


**Figure S5**. Fluorescence emission of L (20 μM) induced by different cations (100 μM) (1-34 are: L, L+$Fe^{3+}$, L+$Na^{+}$, L+$Na^{+}$+$Fe^{3+}$, L+$Cr^{3+}$, L+$Cr^{3+}$+$Fe^{3+}$, L+$Ca^{2+}$, L+$Ca^{2+}$+$Fe^{3+}$, L+$Mg^{2+}$, L+$Mg^{2+}$+$Fe^{3+}$, L+$K^{+}$, L+$K^{+}$+$Fe^{3+}$, L+$Al^{3+}$, L+$Al^{3+}$+$Fe^{3+}$, L+$Mn^{2+}$, L+$Mn^{2+}$+$Fe^{3+}$, L+ $Fe^{2+}$, L+ $Fe^{2+}$+$Fe^{3+}$, L+$Co^{2+}$, L+ $Co^{2+}$+$Fe^{3+}$, L+$Cu^{2+}$, L+$Cu^{2+}$+$Fe^{3+}$, L+$Ni^{2+}$, L+$Ni^{2+}$+$Fe^{3+}$, L+$Zn^{2+}$, L+$Zn^{2+}$+$Fe^{3+}$, L+$Cd^{2+}$, L+$Cd^{2+}$+$Fe^{3+}$, L+$Hg^{2+}$, L+$Hg^{2+}$+$Fe^{3+}$, L+$Pb^{2+}$, L+$Pb^{2+}$+$Fe^{3+}$, L+ $Ag^{+}$ ,L+ $Ag^{+}$+$Fe^{3+}$).

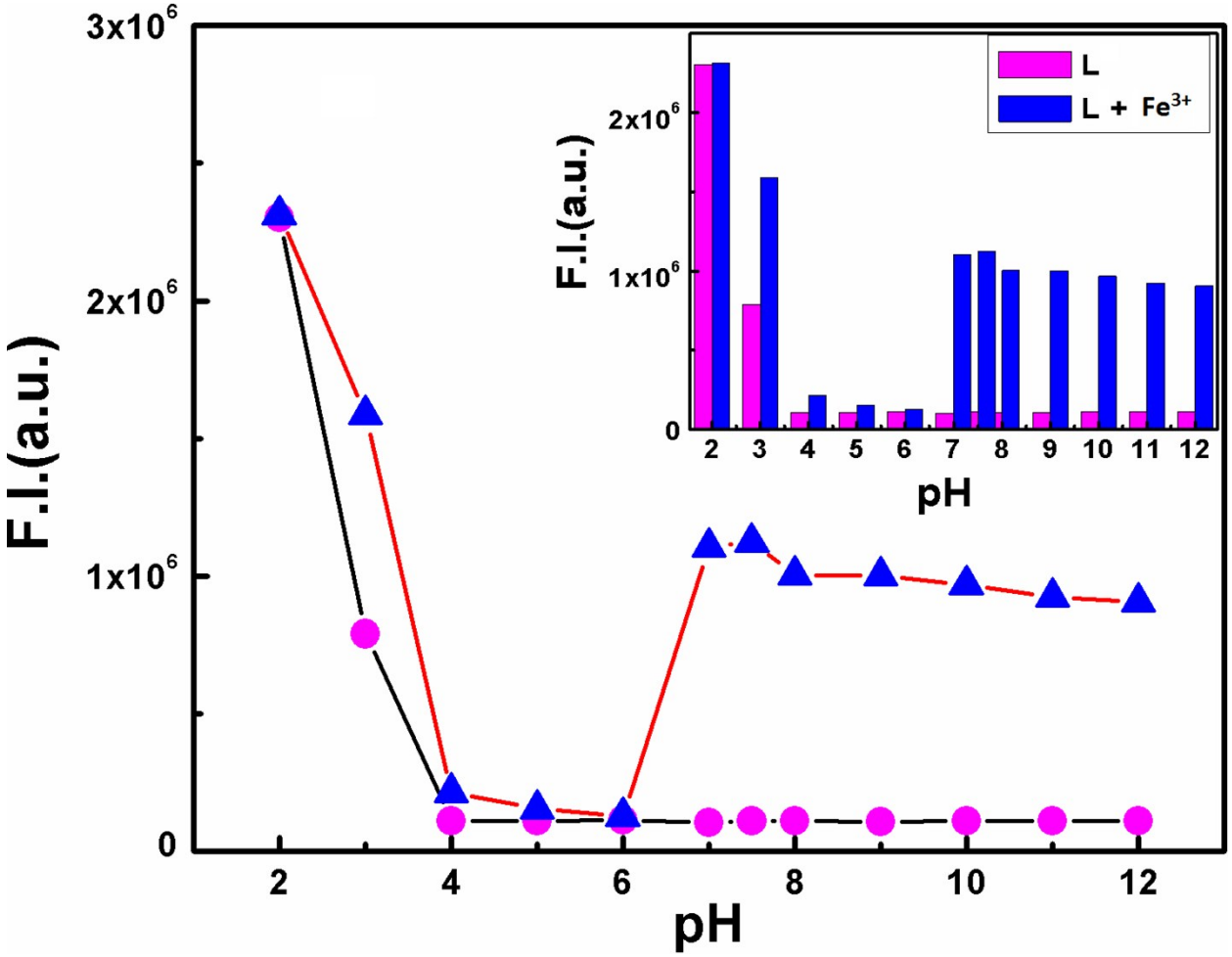


**Figure S6 .** pH dependence of the FIs of the free ligand L (magenta) and the L – $Fe^{3+}$ complex with L:$Fe^{3+}$= 1:1.05 (blue) in the MeCN/$H_2O$ (3:7 v/v) solvent system with $\lambda_{ex}$ = 510 nm. The inset shows the histogram plot

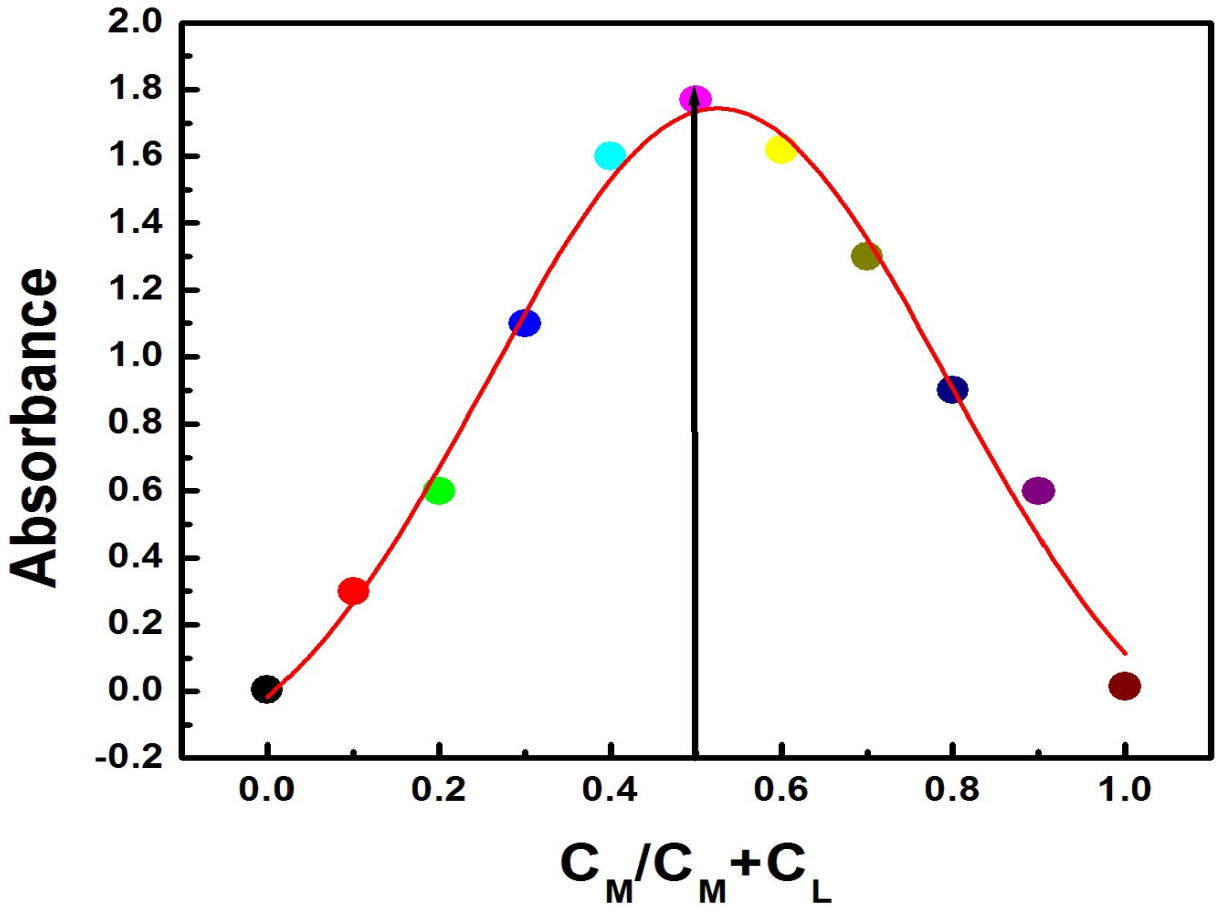


**Figure S7.** Job's plot for the determination of the composition of the L–$Fe^{3+}$ complex.